

RESEARCH OF THE BEST TECHNOLOGICAL AND METALLURGICAL PARAMETERS FOR PERFORMING THE ELECTRIC RESISTANCE WELDING OF LOW CARBON STEELS

C. Mapelli, C. Corna

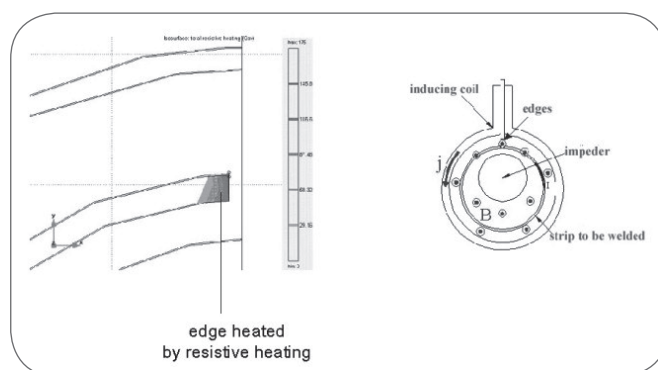
This work deals with the research of the optimal technological and metallurgical parameters in order to implement a reliable procedure for the electric resistive welding of low carbon structural steel, in order to evaluate the conditions which can grant the best mechanical performances. Low carbon steels must be featured by high plastic formability properties, since the production process consists in the piping of a rolled band, followed by an Electric Resistance Welding (ERW) of the edges. The optimal technological parameters have been identified performing welding tests at several levels of electric power, squashing length and forward velocity of the pipe along the coil axis. Several mechanical tests have been performed for the determination of the properties of the materials under examination, in order to characterize the main mechanical properties, i.e. Young modulus, yield and the ultimate stresses, yield point elongation (the strain after which the plastic behaviour takes place), anisotropy coefficients (r_m , Δr), Vickers micro-hardness and hardening coefficient of the materials analysed, while the residual stress induced in correspondence of the welded joining have been determined by X-ray diffraction. The microstructural characteristics of the steels have been obtained through micrographic analyses coupled with the use of Electron Back Scattered Diffraction techniques (EBSD). The value assumed by the hardening coefficient and by the yield elongation point has been revealed to be a strongly significant parameter for assuring the quality of the joining in order to avoid a very early formation of the cracks in the welding region.

Keywords: electric resistive welding, cementite precipitation, hardening coefficient, yield elongation point, residual stresses

INTRODUCTION

This work is about the identification of the best technological parameters of the steel properties which can grant the soundness of pipes realized by ERW high frequency welding. This process is based on the resistive heating of the edges of the steels which cross a volume contained in a coil interested by a current varying at high frequency (500-1000kHz). The time-variant magnetic flow induced by the coils current causes a potential difference and a related current which concentrates on the steel edges producing an intensive and concentrated heating (Fig. 1).

Just after the heating, the strip edges are pulled against themselves by the action of rollers. This is the system through which the welding operation is performed exploiting the High Frequency

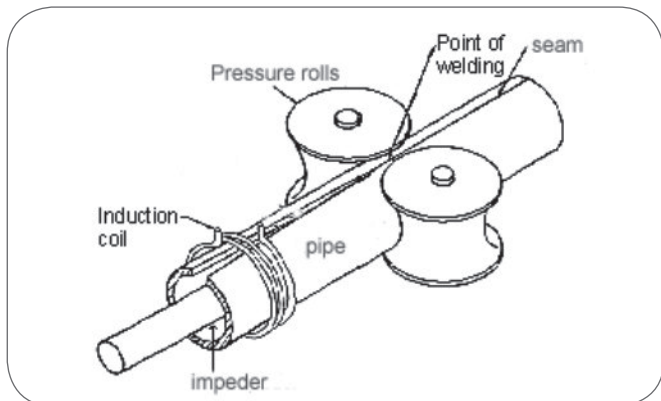


▲
Fig. 1

Example of a simulation showing the layout of the system and the resistive heating produced on the pipe edges to be joined.

Esempio di una simulazione che mostra il layout del sistema e il riscaldamento prodotto sulle estremità del tubo che devono essere saldate.

Carlo Mapelli, Cristian Corna
Sezione Materiali per Applicazioni Meccaniche
Dipartimento di Meccanica, Politecnico di Milano,
via La Masa 34, 20156 MILANO (ITALY)
email: carlo.mapelli@polimi.it



▲
Fig. 2

Layout of a ERW system for pipe production.
Layout del sistema ERW per la produzione dei tubi.



▲
Fig. 3

Example of the complex tubular shape realized by plastic deformation of the welded pipes.
Esempio delle complesse forme tubolari realizzate mediante deformazione plastica dei tubi saldati.

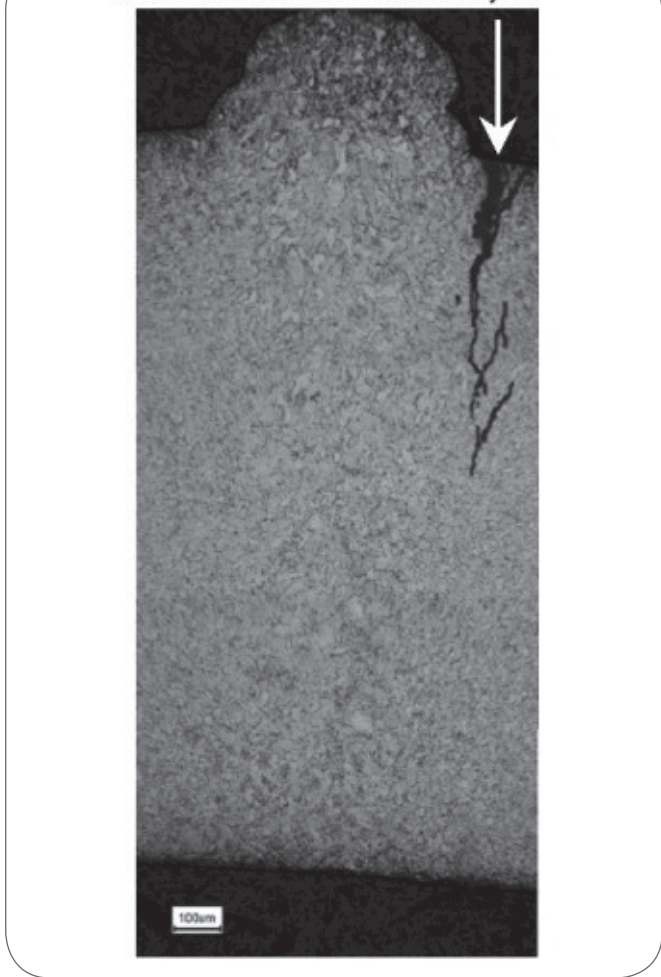
Electric Resistance Welding process: the two metallic edges are pressed by the welding-rollers and brought to fusion by the Joule effect^{1,2,3,4,5,6}(Fig. 2).

The rolled and annealed plates of Low Carbon steels know a wide use for the production of pipes, also for the good formability attitude which can grant the realization of complex shape component through the forming of the welded pipes. The system and the steel characterization are necessary to understand the possible reasons which cause the formation of unacceptable micro-cracks near the seam of the welded steel (Fig. 3), because this type of failure forbids the use of the welded components (Fig. 4, Fig. 5).

EXPERIMENTAL PROCEDURES

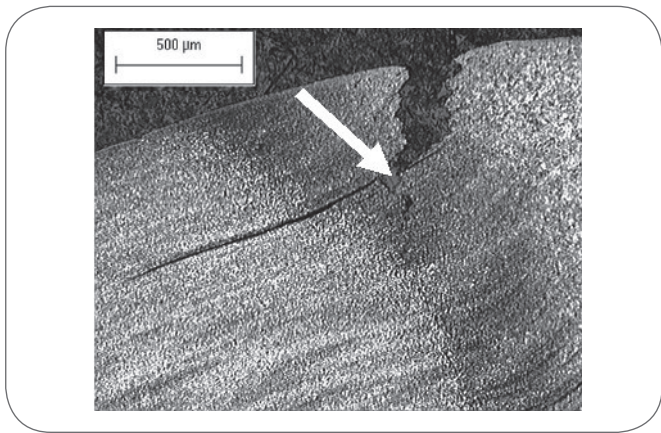
The analysis has been performed on a Low Carbon Steel with a chemical composition largely used, in automotive field, for sport equipment applications etc. (Tab. 1). The welding

Crack revealed near the welded joint



▲
Fig. 4

Example of a micro-crack revealed near the seam region of a welded steel plate.
Esempio di una micro-cricca rivelata vicino alla regione di giunzione.



▲
Fig. 5

Example of a fracture nucleated and grown near non-metallic defects trapped within the seam.
Esempio di una frattura nucleata e propagata in prossimità di inclusioni non metalliche intrappolate all'interno della regione di saldatura.

%wt	C	Mn	Si	S	P	Cr	Ni	Cu	Al	Mo
P1	0.042	0.239	0.012	0.010	0.017	0.0134	0.0153	0.0159	0.055	0.004
P2	0.048	0.224	0.014	0.012	0.010	0.0274	0.0242	0.0319	0.050	0.005

Tab. 1

Average chemical composition of the two examined steels.
Composizione chimica media dei due acciai esaminati.

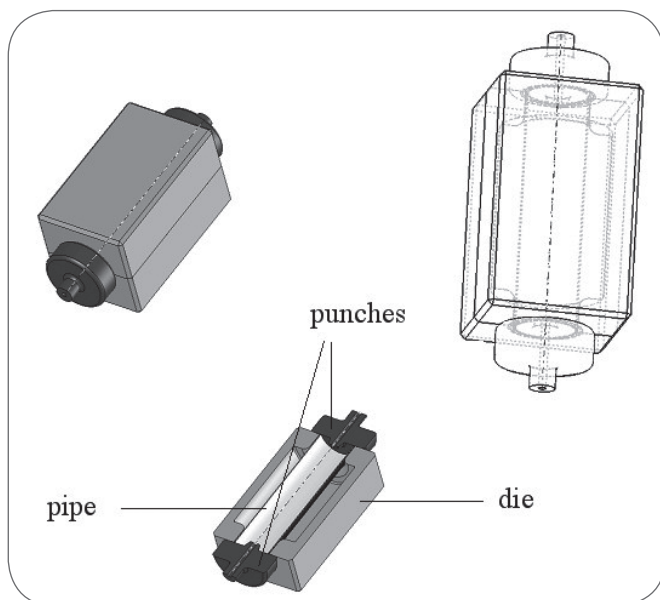


Fig. 6

The hydroforming device used for testing the welded pipes.

Strumento di idroformatura utilizzato per testare i tubi saldati.

experimental trials have been performed on strips 2.0 and 2.5 mm thick (provided by two different suppliers indicated as P1 and P2) in order to point out possible differences produced by the variation of either the chemical composition within the tolerated ranges or in the performed thermo-mechanical processes.

The welding process has been performed in order to produce pipes of 135mm diameter applying different combinations of the operative parameters which can be easily controlled by the operators:

- electric power supply: 210kW-250kW-290kW;
- forwarding velocity: 45m/min-50m/min-55m/min;
- squashing length between the edges: 0.5mm-1mm-1.5mm;

provided a starting distance of pipe edges of 0.2mm. The electric power has been developed applying a frequency of 650kHz. The welding region has been characterized through Vickers micro-hardness profile. Moreover, the analysis of the morphology of the sandglass shape of heat and deformation affected zone (HADZ) and the inclination of the plastic flow deflection lines of this region have been performed. Subsequently, for each combination of the operative parameters, a pipe 50mm long has undergone a hydroforming instrumented test (Fig. 6) through which the water has been pulled into the pipes at a rate of 8MPa/min at room temperature.

The maximum pressure reached during the test has been recorded and assumed as the load which has led the pipe to collapse.

The higher the supported pressure the better the reliability of the welded structure is considered. The hydroforming device has been designed in order to avoid the induction of axial stresses along the pipe wall.

The ERW process imposes significant plastic deformation to the welded edges and this represents a peculiarity of such a welding procedure. The characterization of the main properties of the materials which undergo a plastic deformation process after heating is a fundamental step to identify which is the most important alloy property to be monitored and controlled in order to realize a good and reliable design of the fabrication process. The performed characterization is articulated in:

- chemical analyses, to establish the average composition of the sample;
- metallographic trials to measure the grain size of the steel sample, to detect the different phases, their distribution and the possible presence of particular crystallographic orientation which can affect the mechanical behaviour;
- tensile tests performed along different directions to determine the main mechanical properties (yield stress, ultimate tensile stress, coefficient of hardening, total elongation etc.) and micro-hardness measurements to evaluate the features of heat affected and strained zone near the welding joint;
- X-ray diffraction examination near the welded region in order to point out the residual stresses left by the welding operation.

Chemical Analysis

The chemical analysis of steels supplied by P1 and P2 revealed that P2 material contains a higher concentration of alloying elements, i.e. Ni, Cr and Cu (Tab. 1).

Metallographic Analyses

This step of the analyses was performed for identifying the different phases appearing inside the material, paying particular attention to their sizes, shapes and distributions⁷⁾. In this case the samples have been etched by Picral solution (2÷4g of Picric Acid in 100ml of Ethanol) for 7s in order to point out the presence of the different phases and the grain boundaries. The determination of the grain size has been performed on the realized micrographs according to the UNI 3245 and ASTM E112-82 standards.

The cementite volume fraction featuring the microstructure of the analysed steels has been measured through an automatic image analyser. For each sample an area of 10mm² has been examined.

The Electron Back-Scattered Diffraction (EBSD) probe mounted on a Scanning Electron Microscope (SEM) has been applied for the identification of the crystallographic textures^{8,9,10)}. For this operation the samples, after the grinding and polishing to an average roughness of 0.05µm - operated through the colloidal silica (solution of 80% silica suspended within a 20% H₂O deposited on a rotating titanium disk) - have been inserted within a conductive resin¹¹⁾. The microscope has been set to 20kV and the total scanned surface to obtain the texture measure is of 100mm². The samples used for this analysis are the same investigated for the optical metallographic examination before the application of the etching solution to avoid the alteration of the surface characteristic which can compromise the quality and

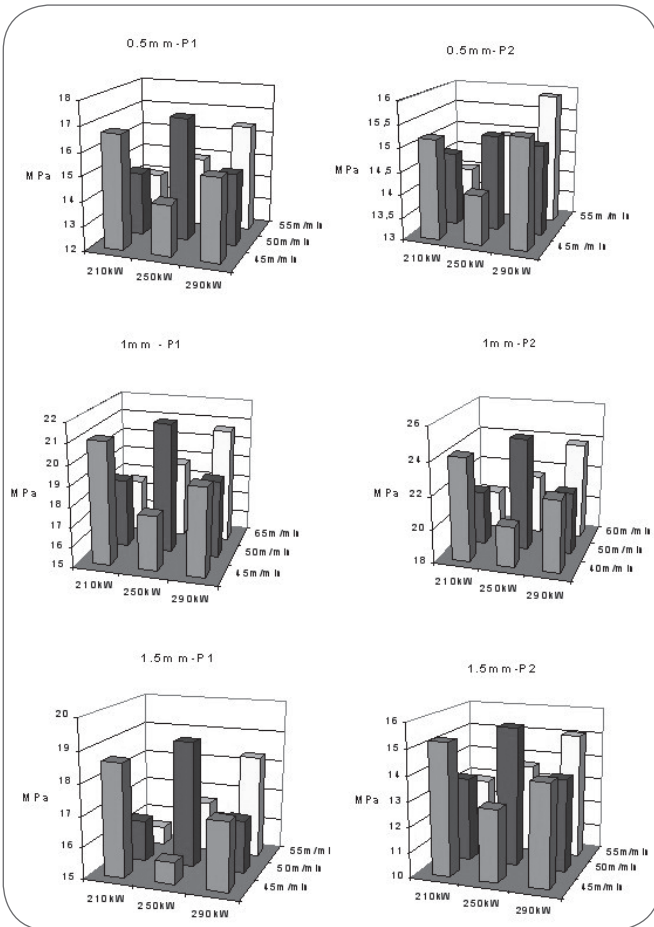


Fig. 7 Maximum water pressure reached in 2.0 mm thick pipe as a function of the squashing length and of the provider.

Massima pressione raggiunta dall'acqua in un tubo di spessore 2.0mm in funzione della lunghezza di schiacciamento e del fornitore.

the reliability of the results obtained through EBSD technique. The analysis of this crystallographic aspect can be useful in order to determine the origin of possible differences revealed in the mechanical behaviour.

Mechanical Analyses

The plates provided for welding were treated through specific thermo-mechanical processes and so they can show significant non isotropic characteristics, then the characterization of their mechanical properties has been carried out along different directions.

The characterization was performed through tensile tests applying an elongation velocity of 25mm/min according to UNI EN 10002 which allowed to measure the Young modulus, the yield and the ultimate tensile stresses, the yield point elongation (YPE) (the elongation at which the steel begins to flow plastically) and the hardening coefficient of the material (n) according to ASTM E646-00, which can be derived making a logarithmic linearization of the Hollomon equation^{12,13}:

$$\sigma = K \varepsilon_p^n \rightarrow \ln \sigma = \ln K + n \ln \varepsilon_p \quad (1)$$

where ε_p represents the plastic component of the deformation.

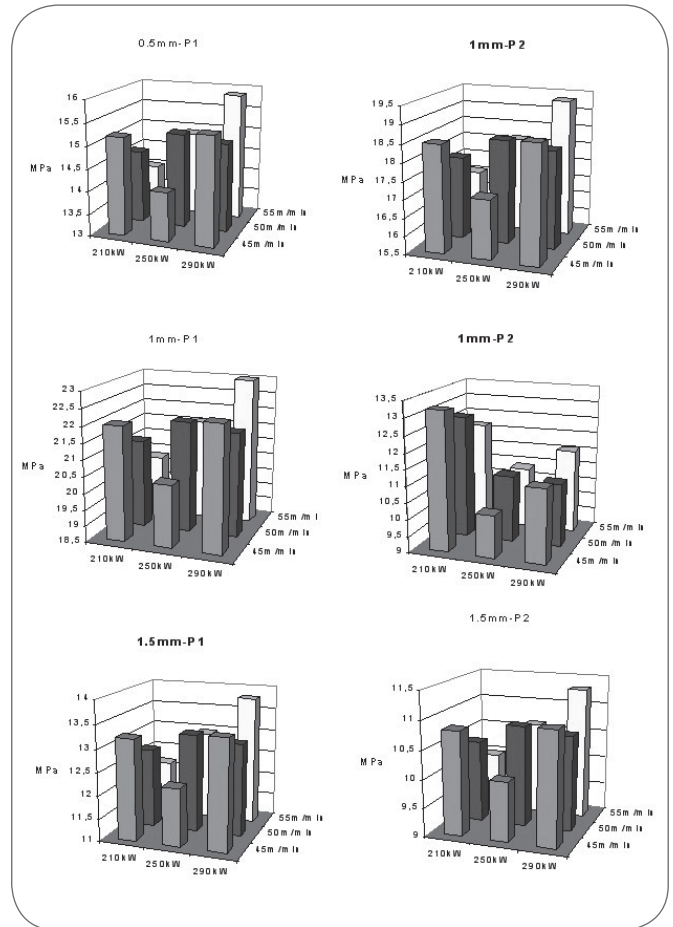


Fig. 8 Maximum water pressure reached in 2.5mm thick pipe as a function of the squashing length and of the provider.

Massima pressione raggiunta dall'acqua in un tubo di spessore 2.5mm in funzione della lunghezza di schiacciamento e del fornitore.

As already anticipated, materials which undergo a rolling process show anisotropy in the mechanical behaviour, so the tensile specimens have been sampled along the three main characteristic directions rotated of 0, 45, 90° from the rolling one. For each sample two tensile specimens for each orientation have been considered. In order to obtain the average parameters which can describe this anisotropy the mechanical properties measured along the different directions have been reduced to an average synthetic form:

$$X_m = \frac{X_0 + 2X_{45} + X_{90}}{4} \quad (2)$$

The subscripts represent the angles of misalignment from the rolling direction. For the analysis of these parameters related to the anisotropy two samples have been tested for each direction for the plate with a thickness of 2mm and for the one with a thickness of 2.5mm. In the rolled products other interesting parameters to be taken into account are the average normal anisotropy coefficient r_m and the planar anisotropy Δr ^{14,15} according to ASTM E517-00. The measurements of the anisotropy parameters have been performed after the application of a 10% strain.

		210kW	250kW	290kW
Squashing length 1mm	40m/min			
	50m/min			
	50m/min			
Squashing length 1.5mm	40m/min			
	50m/min			
	60m/min			
Squashing length 0.5mm	40m/min			
	50m/min			
	50m/min			

Fig. 9

Morphology of the welded zone in 2.5mm thick pipes with steel provided by P1.

Morfologia della zona saldata in un tubo di spessore 2.5mm fornito da P1.

The presence of a possible Heat Affected Deformed Zone (HADZ) has been evaluated through the determination of Vickers micro-hardnesses (ASTM E384) across the welded joint, in which the measurements have been performed with a step of 50µm between two successive measurements and applying a load of 25g for 15s.

Determination of the residual stresses

Using an X-Ray diffractometer (X-Stress 3000) and varying the work angle between -45° and +45°, the measurement of the residual stresses inside the material has been performed: the diffractometer provides the values of the two stresses σ_1 and σ_2 and the amplitude of the angle ϕ , representing the rotation between the stresses measured along the fixed reference system and the direction of the principal stresses (σ, τ). These quantities can be opportunely elaborated to give the value of the Von Mises equivalent stress:

$$\sigma_{VM} = \sqrt{\sigma^2 + 3\tau^2} \quad (3)$$

where

$$\sigma = \frac{\sigma_1 + \sigma_2}{2} + \left(\frac{\sigma_1 - \sigma_2}{2} \right) \cos(2\phi) \quad (4)$$

$$\tau = \left(\frac{\sigma_1 - \sigma_2}{2} \right) \sin(2\phi) \quad (5)$$

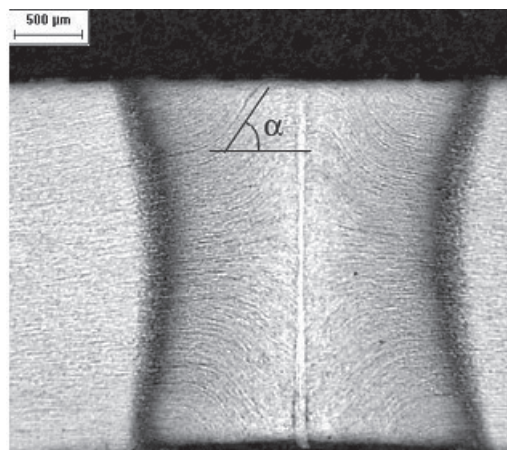


Fig. 10

Example of the revealed deflection lines of plastic flow revealed on a welding performed through the correct combination of the technological parameters.

Esempio delle linee di deflessione associate al flusso plastico rivelate su una saldatura effettuata con il settaggio ottimale dei parametri tecnologici.

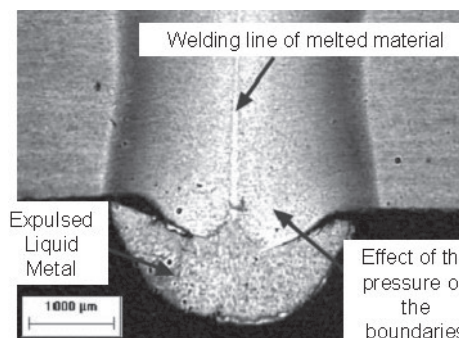


Fig. 11

Example of dirty materials and oxides pulled out from the welded joining by the squashing movement.

Esempio dello sporco e degli ossidi estratti dal giunto saldato durante il movimento di squashing.

RESULTS AND DISCUSSION

The highest resistance level to the hydroforming pressure has been reached for 1mm pulling length and this implies (provided an initial edge distance of 0.2mm) that the squashing penetration between the pulled edges is of 0.8mm (Fig. 7, Fig. 8, Fig. 9). This distance seems fundamental to grant a correct symmetry of the sandglass shape of HADZ and the average deflection angle of 35.1° (st.dev. ±3.1°) at the middle of thickness and of 78.3° (st.dev. ±2.9°) near the surface in order to assure an efficient removal of the defects produced by the presence of oxides or dirty residuals (Fig. 10, Fig. 11). At the same time the largest

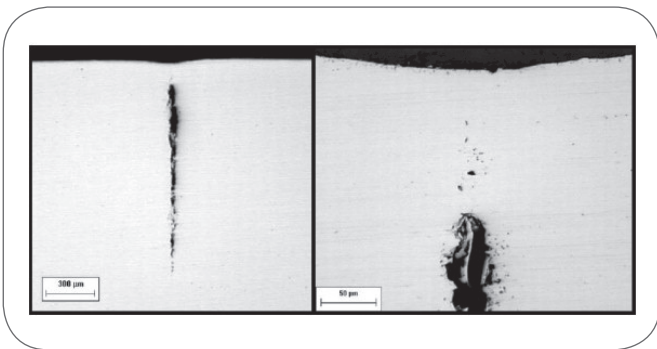


Fig. 12
Examples of defects trapped within the welding and the absence of regular continuity within the joining associated with the lowest level of squashing.

Esempio dei difetti intrappolati all'interno della saldatura e dell'assenza della regolare continuità in corrispondenza delle giunzioni associate ai livelli più bassi di squashing (schiacciamento).

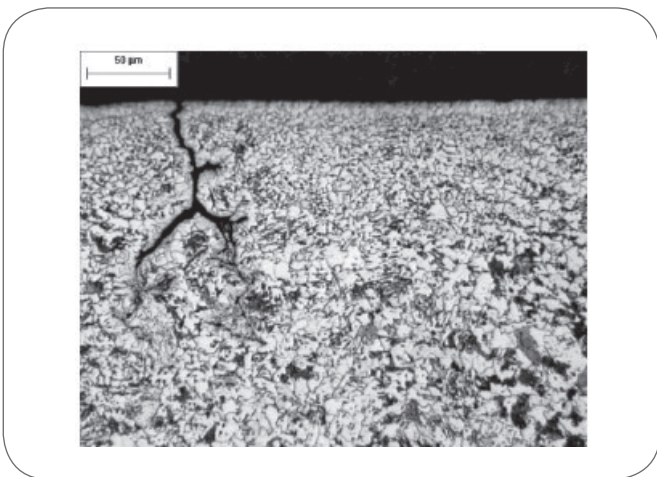


Fig. 13
Example of a fracture developed on the welded pipe.
Esempio di una frattura sviluppatasi sul giunto saldato.

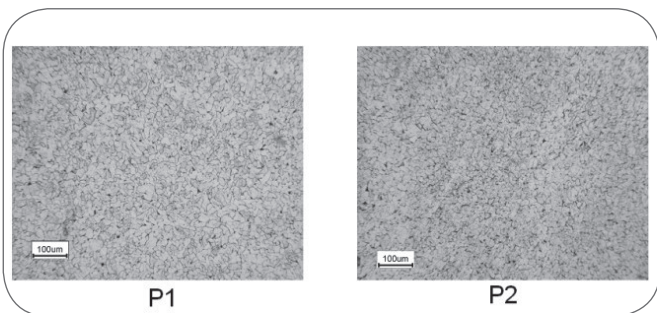


Fig. 14
Example of the grains featuring two steels provided by P1 and P2.
Esempio della microstruttura caratteristica dei due acciai forniti da P1 and P2.

squashing (1.5mm) seems to cause an excessive distortion of the sandglass shape which is always associated with unacceptable damage of the seam or of the adjacent region (Fig. 9).

The lowest value of the squashing length does not grant the complete expulsion of the defects and this is proved by the values assumed by the deflection angle of 23.1° (st.dev. $\pm 4.3^\circ$) at the middle of thickness and 47.1° (st.dev. $\pm 5.1^\circ$), near the surface, which does not seem enough to assure the removal of the defect and a strong and reliable welded junction (Fig. 9, Fig. 12).

Once identified the most favourable squashing length, it is possible to search the correct combination of electric power supply and forwarding velocity. The more promising combinations seem to be:

- 210kW for 45m/min;
- 250kW for 50m/min;
- 290kW for 55m/min.

This indicates that the specific energy for unit length to be welded is included between 280kJ/m and 316kJ/m.

On the other hand, difference shown by the steels produced by different providers demonstrate that the correct individuation of the technological parameters is not enough for maximizing the mechanical performances of the welded pipes. Actually, the pipes produced using the steel provided by P2 show systematically worse performances than the ones provided by P1. Thus, micro-structural investigations can cast a further light to assure a better quality level.

The surface developments of the cracks are always parallel to the welding seam (Fig. 4, Fig. 13).

The P1 steel shows slightly coarser grains than P2 one and so these steels present different values of the grain size ASTM coefficient (9 and 10, respectively) (Fig. 14).

The amount of cementite (Fe_3C) precipitated on the grain boundaries in P2 steels is of 31% greater than the one featuring the P1 microstructure (Fig. 15); this precipitation allows the enhancement of the hardness of the material but causes, at the same time, increase in the brittleness and a loss in the plastic formability of the steel (Tab. 2).

The texture analysis^{16,17,18,19} points out the presence of com-

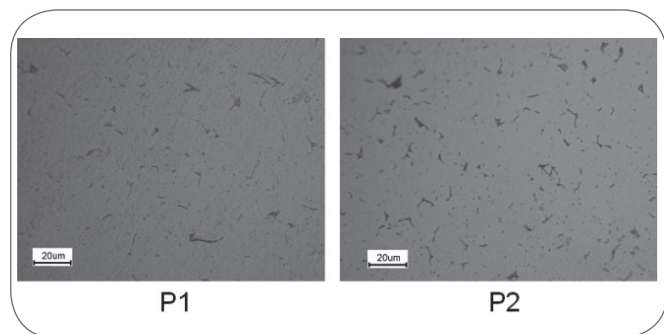


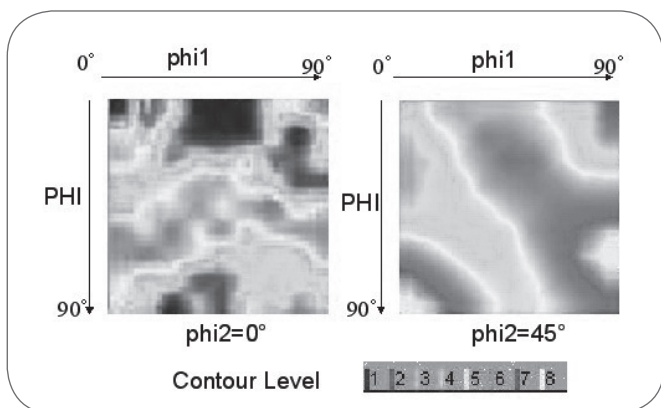
Fig. 15
Example of the characteristic difference in the features of the cementite precipitates present in steels provided by P1 and P2. In the P1 steel the cementite precipitates are less and less coarse than in P2 steel.
Esempio delle tipiche differenze nelle caratteristiche della cementite precipitata negli acciai forniti da P1 and P2: nell'acciaio P1 i precipitati sono inferiori in numero e meno grossolani rispetto all'acciaio P2.

	E(GPa)	Yield stress (MPa)	Yield point of elongation (%)	r_m	Δ_r	n
P1 2mm	205	300	4	0.91	-0.09	0.22
P1 2.5mm	189	275	4.5	0.94	-0.13	0.2
P2 2mm	202	303	3.6	0.93	-0.1	0.15
P2 2.5mm	207	325	3	0.93	-0.18	0.14

▲ Tab. 2

Main average mechanical characteristics revealed by the tensile tests.

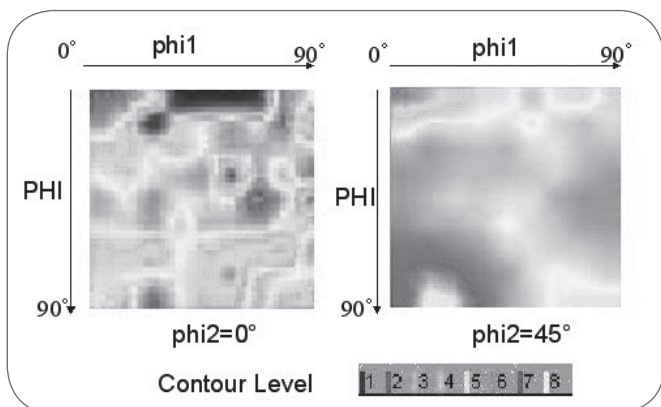
Valori medi delle principali caratteristiche meccaniche misurate mediante prove di trazione.



▲ Fig. 16

Main textures pointed out by the ODF diagram section on correspondence of (a) $\phi_2 = 0^\circ$ and (b) $\phi_2 = 45^\circ$ at the middle of the thickness in steel 2.5mm thick provided by P1.

Principali tessiture emerse dalla sezione del diagramma ODF in corrispondenza di (a) $\phi_2 = 0^\circ$ e (b) $\phi_2 = 45^\circ$ a metà profondità in un acciaio dello spessore di 2.5mm fornito da P1.



▲ Fig. 17

Main textures pointed out by the ODF diagram section on correspondence of (a) $\phi_2 = 0^\circ$ and (b) $\phi_2 = 45^\circ$ at the middle of the thickness in steel 2.5mm thick provided by P2.

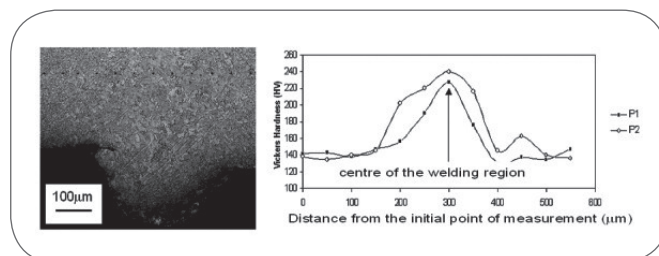
Principali tessiture emerse dalla sezione del diagramma ODF in corrispondenza di (a) $\phi_2 = 0^\circ$ e (b) $\phi_2 = 45^\circ$ a metà profondità in un acciaio dello spessore di 2.5mm fornito da P2.

ponents particularly suitable for a plastic deformation process, actually a prominence of the components in γ -fibre in all the samples under examination has been revealed; the only difference is the greater dispersion of components featuring the P2 samples, joined together with a lower intensity of favourable textures characterized by the planes {111} and {110} of the body centred cubic lattice lying parallel to the rolling plane (Fig. 16, Fig. 17). Moreover, P2 steel shows a more intense {001}<100> Cube component which is usually detrimental for the formability attitude. Thus, this situation can cause a worse formability attitude, which seems to produce considerable variation on the hardening coefficient.

The tensile tests carried out indicated that P2 steels are featured by higher values of Young modulus and yield stress, if compared to the values typical of P1 materials (Tab. 2). On the contrary, P1 steels present yield point elongations slightly higher than P2 ones, even if the values are very close and correspond to few percents. The presence of significant yield point elongation is a peculiarity of the low carbon steels and it can represent a ductility parameter of the material, although an excessive value of this parameter may cause the appearance of the so called 'Lüders bands' on the surface and on the layer immediately under it. This phenomenon can be detrimental for the surface quality of the component, but in this case the performed industrial trials have not revealed this problem.

The average normal anisotropy parameter (r_m) and the one describing the planar anisotropy (Δ_r) turned out to be practically similar in all the analysed samples and the difference pointed out cannot be the responsible for the formation of the micro-cracks developed in P2 steel.

On the contrary, the hardening coefficient and the yield elongation point assume significantly higher values in the steels provided by P1 than in the ones from P2. Thus, this parameter seems to cover an important role in order to avoid the start up and the development of the cracks



▲ Fig. 18

Example of the comparison of the average measured micro-hardness profile in the steel provided by P1 and P2.

Esempio del confronto dei profili medi di microdurezza negli acciai forniti da P1 e P2.

P1				
n° of test	1	2	3	4
sigma 1 (MPa)	358	129	138	257
sigma 2 (MPa)	34	-3	48	110
Phi	-85	0	31	40
Average Von Mises Stress 118MPa				
P2				
n° of test	1	2	3	4
sigma 1 (MPa)	236	168	107	118
sigma 2 (MPa)	-77	57	80	20
Phi	2	-121	2	-37

▲
Tab. 3

Measured residual stress measured in the region where the micro-cracks usually take place.
Sforzi residui misurati nella regione dove generalmente si sviluppano le microcricche.

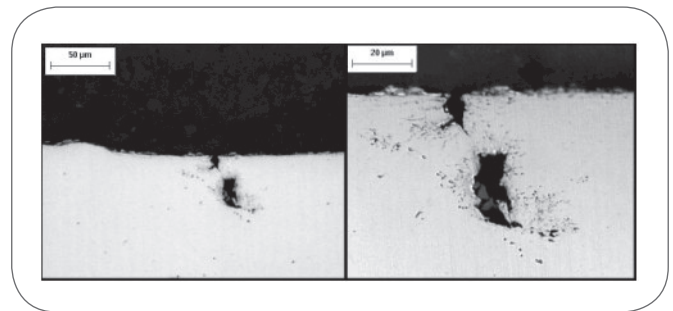
near the welding seam. The Vickers micro-hardness profile measured on the welding reveals a hardness of about 220-240HV and a slightly higher value in the region just adjacent to the seam and more pronounced in the steel provided by P2, probably due also to a larger carbide precipitation (Fig. 18). The value of hardness measured in HADZ are extremely high if compared to the base material ones featured by average values included between 120-140HV. Provided that the melted and solidified region is averagely around 40 μ m, the increase to around 220-240HV revealed for about 200 μ m on the two sides of the seam appears to be largely caused not only by heating but also by the hardening process due to the performed plastic straining.

The analyses realized using the X-Ray diffractometer confirmed this statement, revealing that P1 steels show average higher residual stresses, if compared to welded steels provided by P2 [233MPa (P1) vs. 118MPa (P2)] (Tab. 3). The most plausible explanation of this phenomenon could be the partial relax of the stresses produced by the formation even of micro-cracks in the region adjacent the welding seam.

Thus, the results of the performed analysis pointed out that the significant difference are related to:

- the chemical composition of the steel;
- the amount of the cementite precipitation on the grain boundaries;
- the values assumed by the hardening coefficient;
- the relaxation residual stresses produced by the welding system.

These aspects can play a cooperative role in the production of the revealed damage of the welded structure. The most reliable explanation of the failure process can be summarized in this way: when the compression produced by the rolls between the sides to be welded is removed, the welded pipe undergoes a displacement due to the elastic return which produces a stress on the welded seam and on the adjacent regions. These residual stresses produce some strains in the steels which are higher when the hardening coefficient is lower. Actually, a high hardening coefficient contains the deformation produced by the residual stresses. If the hardening coefficient is low enough to cause a deformation which is over the maximum local strain acceptable



▲
Fig. 19

Example of micro-fracture revealed in steel provided by P2 featured by a lower residual stress.
Esempio di una microfrattura rivelata nell'acciaio fornito da P2 e caratterizzato da un basso livello degli sforzi residui.

by the material, this gives rise to the cracks. The formation of cracks relaxes the induced residual stress and this can explain the lowest values found in the cracked steels. On the other hand, the chemical composition and the related cementite precipitation seem to play an important role too, because the presence of elements which increase the carbide formation, i.e. chromium, increases the hardness and decreases the ductility of steel which is more sensitive to the cracks induced by the strain caused by the welding stresses. Thus, a high yield point of elongation, a high hardening coefficient and a chemical composition not prone to the carbide precipitation seem to be the most important parameters for a correct realization of the ERW process to produce tubular structure.

CONCLUSIONS

The production of pipes featured by a correct soundness through the ERW process can take advantage by the control of the technological parameters: a squashing length of 1 mm starting from a distance of 0.2 mm associated to an energy supply per unit length included in the range of 280kJ/m and 316kJ/m seems to represent an optimal combination.

On the other hand, at least two further important aspects related to the selection of the material need to be taken into account. The first aspect is the choice of a steel with a contained tendency to the precipitation of carbides, because this avoid an excessive lowering of the ductility of the steels; on the other hand, this is a factor always taken into account for all the welding process. A second important aspect, that can be added also to the procedure of quality control of the starting base material is granting high enough hardening index and yield elongation point, because they can decrease the plastic strain induced by the residual stresses left by the welding system within the steel structure.

REFERENCES

- [1] R.K.Nichols: 'High frequency welding, the process and the applications', Proceeding of International Tube Conference, 1999;
- [2] R.K.Nichols: 'High frequency: pipe and tube welding', Proceedings International Tube Conference, 1994;
- [3] P.F. Scott: 'Key parameters of high frequency welding', Proceedings of the Tube&Pipes Congress 1996, Dusseldorf, Germany, 1996;

[4] J. W. Elmer, T. A. Palmer, W. Zhang, B. Wood and T. De-
bRoy: *Acta Mater.*, 51 (2003), 3333.
[5] B. H. Chang and Y. Zhou: *J. Mater. Process. Technol.*, 139
(2003), 635.
[6] A. De, L. Dorn and O. P. Gupta: *Sci. Technol. Weld. Join-
ing*, 5 (2000), 49;
[7] Y. Watanabe and I. Momose: *Ironmaking Steelmaking*,
31 (2004), 265;
[8] Internet site: www.ebsd.com;
[9] W. B. Hutchinson and M. Hatherley: *An Introduction to
Texture in Metals*, Monograph 5, The Institution of Metal-
lurgists, London, (1979), 255.
[10] U. F. Kocks, C. N. Tomè and H.-R. Wenk: *Texture and
Anisotropy*, Cambridge University Press, Cambridge,
(2000), 421;
[11] W. F. Hosford and R. M. Caddell: *Metal Forming: Me-
chanics and Metallurgy*, 2nd Ed., PTR Prentice Hall, New
York, (1993), 286
[12] R. K. Ray, J. J. Jonas and R. E. Hook: *Int. Mater. Rev.*, 39
(1994), 129;
[13] Standard UNI EN 10002, 'Materiali metallici: prova di
trazione a temperatura ambiente' (1992);
[14] Standard ASTM E517-00: 'Standard test method for pla-
stic strain ratio for sheet metal' (August 2000);
[15] W. T. Lankford, S. C. Snyder and J. A. Bauscher: *Trans.
Am. Soc. Met.*, 42 (1950), 1197.
[16] M. R. Barnett: *Modern LC and ULC Sheets Steels for
Cold Forming: Processing and Properties*, ed. by W. Bleck,

Aachen University of Technology, Aachen, (1998), 61;
[17] M. R. Barnett and J. J. Jonas: *ISIJ Int.*, 39 (1999), 856;
[18] H. J. Bunge: *Texture Analysis in Materials Science-Ma-
thematical Methods*, Butterworths, London, (1982), 145;
[19] U. F. Kocks, C. N. Tomè and H.-R. Wenk: *Texture and
Anisotropy*, Cambridge University Press, Cambridge,
(2000), 421.

LIST OF SYMBOLS

E	Young modulus [GPa]
r_m	average normal anisotropy coefficient
Δr	planar anisotropy coefficient
K	coefficient of strengthening in the Hollomon relation [MPa]
n	hardening coefficient
σ_{VM}	Von Mises Equivalent Stress [MPa]
ϵ_w	width deformation
ϵ_t	thickness deformation
ϵ_p	plastic component of the deformation
l_0	initial length of the specimen used for the tensile test [m]
l_f	final length of the specimen used for the tensile test [m]
r	normal anisotropy coefficient
r_m	average normal anisotropy coefficient
X_m	average value of the generic mechanical parameter X
X_n	value of the generic mechanical parameter X along a direction rotated by n from the rolling direction
w_0	initial width of the specimen used for the tensile test [m]
w_f	final width of the specimen used for the tensile test [m]

ABSTRACT

RICERCA DEI PARAMETRI TECNOLOGICI E METALLURGICI OTTIMALI PER L'ESECUZIONE DELLA SALDATURA PER RESISTENZA ELETTRICA DEGLI ACCIAI A BASSO CARBONIO

*Parole chiave: saldatura per resistenza elettrica, preci-
pitazione della cementite, coefficiente di incrudimento,
deformazione allo snervamento, sforzi residui*

Il presente lavoro tratta la ricerca dei parametri tecnologici e metallurgici ottimali per implementare un processo affidabile di saldatura elettrica per resistenza degli acciai strutturali a basso tenore di carbonio (Tabella 1) e per stabilire le condizioni in grado di garantire le migliori prestazioni dal punto di vista meccanico. Gli acciai in esame devono possedere elevate capacità di deformazione plastica in quanto il processo produttivo prevede l'avvolgimento di un nastro laminato, seguito dalla saldatura delle estremità per resistenza elettrica (ERW – Electric Resistance Welding) (Figure 1 e 2). I parametri tecnologici ottimali sono stati evidenziati mediante

l'esecuzione di test di saldatura a diversi livelli di potenza elettrica, lunghezza di schiacciamento e velocità di avanzamento del tubo lungo gli assi delle bobine. Per la misura delle proprietà del materiale considerato sono stati eseguiti diversi test meccanici allo scopo di caratterizzare le principali proprietà meccaniche, quali il modulo di Young, i carichi di snervamento e di rottura, l'allungamento al punto di snervamento (lo sforzo oltre il quale comincia il comportamento plastico), i coefficienti di anisotropia (r_m , Δr), le microdurezze Vickers e i coefficienti di incrudimento (Tabella 2); gli sforzi residui indotti in corrispondenza dei giunti saldati sono stati determinati per mezzo della diffrazione di raggi X (Tabella 3). Le caratteristiche microstrutturali degli acciai sono state ottenute attraverso analisi micrografiche accoppiate all'utilizzo di tecniche di diffrazione EBSD (diffrazione degli elettroni retrodiffusi) (Figure 16 e 17). Si è riscontrato che i valori dei coefficienti di incrudimento e dei punti di yield elongation sono da ritenersi un parametro particolarmente significativo per assicurare la qualità della saldatura ed evitare la prematura formazione di cricche in prossimità dei giunti saldati (Figure 13 e 19) a seguito delle operazioni di compressione o espansione sulle superfici laterali dei tubi.